

Finite temperature effects in trapped Fermi gases with population imbalance

Chih-Chun Chien, Qijin Chen, Yan He, and K. Levin

James Franck Institute and Department of Physics, University of Chicago, Chicago, Illinois 60637, USA

(Received 28 May 2006; published 24 August 2006)

We study the finite temperature T behavior of trapped Fermi gases as they undergo BCS–Bose–Einstein condensation (BEC) crossover, in the presence of a population imbalance. Our results, in qualitative agreement with recent experiments, show how the superfluid phase transition is directly reflected in the particle density profiles. We demonstrate that at $T \neq 0$ and in the near-BEC and unitary regimes, the polarization is excluded from the superfluid core. Importantly, a substantial polarization fraction is carried by a normal region of the trap having strong pair correlations, which we associate with noncondensed pairs or the “pseudogap phase.”

DOI: [10.1103/PhysRevA.74.021602](https://doi.org/10.1103/PhysRevA.74.021602)

PACS number(s): 03.75.Hh, 03.75.Ss, 74.20.–z

Recent work [1–3] on trapped atomic Fermi gases with population imbalance has become particularly exciting. With the application of a magnetic field, these systems exhibit an evolution [4–6] from BCS to Bose–Einstein condensation (BEC). Not only are these gases possible prototypes for condensed matter systems [7,8] in the presence of a magnetic field and Zeeman coupling, but they may also be prototypes for particle and nuclear physics systems [9,10]. These pioneering experiments have been done by two experimental groups [1,2].

There are a number of key experimental observations which we now list. (i) Both groups have observed that the trap profiles are characterized by a central core of (at most) weakly polarized superfluid, surrounded [3] by a *normal region where the bulk of the polarization is contained*. (ii) The normal region appears to consist of overlapping clouds of both spin states (“normal mixture”), followed at the edge of the cloud by a region consisting only of the majority component.

These population imbalance experiments have been done [1,3] in conjunction with other measurements (vortex excitations and magnetic field sweeps) which establish the presence and the location for superfluid condensation. (iii) Even more recently [3] it has been demonstrated that the presence of superfluidity at and below T_c is directly reflected in changes in the shape of the clouds. (iv) Important for the present purposes is the fact that [3] there are strong interaction effects within the normal region of the cloud, which have not yet been incorporated in the theoretical literature [11,12].

The goal of the present paper is to address the four points [(i)–(iv)] listed above through a finite temperature theory of BCS-BEC crossover in the presence of population imbalance within a trap. A related study of the homogeneous system was presented earlier [13]. What is unique to our work is the capability of separating in a natural way the condensed from noncondensed pair contributions to the trap profile; this is complicated by the fact that (except at $T=0$) the presence of a fermionic excitation gap is *not* a signature of phase coherent superconductivity. We also present calculations of T_c in a trap and show how the general shape of the profile changes below and above T_c , unlike what is found experimentally and theoretically [14] in the absence of polarization. In a related fashion, we examine the noncondensed pair states in the trap and determine to what extent they differ from a free gas mixture of the two spin states.

Our principal findings are at low $T \neq 0$ and for the unitary and near-BEC regimes: (a) the superfluid core seems to be robustly maintained at nearly zero polarization, and (b) the mixed normal region carries a significant fraction of the polarization within a nonsuperfluid state having strong pair correlations. Indeed, experiments suggest [3] that “even in the normal state, strong interactions significantly deform the density profile of the majority spin component.” Here we interpret these correlations as noncondensed pairs which have no counterpart at $T=0$ and which are associated with an excitation gap (“pseudogap”) in the fermionic spectrum. Finally, (c) in the course of making contact with points (i)–(iv) listed above we show good qualitative agreement with the experiment.

Because we restrict our attention to condensates (and their pseudogap phase counterparts) with zero momentum ($q_0=0$) pairing, we do not explore those regimes of the phase diagram corresponding to the lowest temperatures, and highest polarizations. Recent, very nice theoretical work based on the Bogoliubov–de Gennes (BdG) approach [15,16] has shown that in the *ground* state at unitarity, the $q_0 \neq 0$ Fulde-Ferrell-Larkin-Ovchinnikov (FFLO) state [17] must be incorporated. The polarization in this state at $T=0$ tends to appear at the edge but *within the condensate* [16]. Fortunately, the present work provides a good indication of where the FFLO phase will enter, since it occurs when the $q_0=0$ phase is found to be unstable [16,18].

The value of the present work derives from the fact that a central theme in the experimental literature involves distinguishing the condensate from the normal regions of the trap. The precise nature of the normal (N) and superfluid (S) phases are all of great interest and one needs a theory which distinguishes N from S at finite temperatures, where the excitation gap is no longer a signature of superfluidity. Previous theoretical approaches, based on the BdG [15,16] and local density approximation (LDA) [11,12,19,20] schemes have emphasized $T=0$, albeit without reaching any clear consensus. The inclusion of finite T for the LDA case has been introduced within the same formalism we use here [8], but without separating the condensed and noncondensed pair contributions. In addition the application of BdG to $T \neq 0$ is viewed as problematic because it does not incorporate noncondensed pairs [5,21,22]. At the same time, it should be stressed that this BdG approach [15,16] is most likely the appropriate way to get a full picture of the $T=0$ phase.

The formalism used in this paper was outlined earlier [13]. Here we incorporate trap effects by use of the LDA. We adopt a one-channel approach since the ${}^6\text{Li}$ resonances studied thus far are broad and consider a Fermi gas of two spin species with kinetic energy $\epsilon_{\mathbf{k}} = \hbar^2 k^2 / 2m$ subject to an attractive contact potential ($U < 0$) between the different spin states. We define $\delta n = n_{\uparrow} - n_{\downarrow} > 0$, where $n = n_{\uparrow} + n_{\downarrow}$ is the total atomic density. Importantly, we include [23] noncondensed pairs at general T . The T matrix or noncondensed pair propagator is $t(Q) = U / [1 + U\chi(Q)]$, where $\chi(Q)$ is the pair susceptibility which depends self-consistently on the fermionic excitation gap Δ . The presence of pairing correlations means that Δ^2 contains two additive contributions from the condensed (Δ_{sc}^2) and noncondensed pairs (Δ_{pg}^2). In the superfluid phase, we have $1 + U\chi(0) = 0$, equivalent to $\mu_{pair} = 0$, the BEC condition of the pairs. As a consequence, the equations become simpler below T_c and we may expand the T matrix to arrive at a characteristic frequency $\Omega_{\mathbf{q}} = \hbar^2 q^2 / 2M^*$ which characterizes the dispersion of the noncondensed pairs. These incoherent pair excitations are different from the linearly dispersing order parameter collective modes [24].

We now summarize the self-consistent equations [14,23], in the presence of a spherical trap, treated at the level of LDA with trap potential $V(r) = \frac{1}{2}m\omega^2 r^2$. Within LDA, an elongated trap used in experiment can be mapped onto the spherical case. T_c is defined as the highest temperature at which the self-consistent equations are satisfied precisely at the center. At a temperature $T < T_c$, the superfluid region extends to a finite radius R_{sc} . The particles outside this radius are in a normal state, with or without a pseudogap.

The generalized local gap equation is given by

$$\frac{m}{4\pi a} = \sum_{\mathbf{k}} \left[\frac{1}{2\epsilon_{\mathbf{k}}} - \frac{1 - 2\bar{f}(E_{\mathbf{k}})}{E_{\mathbf{k}}} \right] + Z\mu_{pair}, \quad (1)$$

where $\mu_{pair}(r) = 0$ in the superfluid region $r \leq R_{sc}$, and must be determined self-consistently at larger radii. The quantity Z is the inverse residue of the T matrix [13]. For convenience we write $\bar{f}(x) \equiv [f(x+h) + f(x-h)]/2$, where $f(x)$ is the Fermi distribution function. Here we set $\hbar = 1$, and use $m/4\pi a = 1/U + \sum_{\mathbf{k}} (2\epsilon_{\mathbf{k}})^{-1}$ to regularize the contact potential, where a is the two-body s -wave scattering length. The dispersion is given by $E_{\mathbf{k}} = \sqrt{[\epsilon_{\mathbf{k}} - \mu(r)]^2 + \Delta^2}$, with $\mu(r) = (\mu_{\uparrow} + \mu_{\downarrow})/2 - V(r)$. We also define the r -independent parameter $h = (\mu_{\uparrow} - \mu_{\downarrow})/2$. Since $\delta n \geq 0$, we always have $h > 0$. More generally, μ_{σ} is the chemical potential for spin σ at the trap center.

The local pseudogap contribution (present only at $T \neq 0$) to $\Delta^2(T) = \Delta_{sc}^2(T) + \Delta_{pg}^2(T)$ is given by

$$\Delta_{pg}^2 = \frac{1}{Z} \sum_{\mathbf{q}} b(\Omega_{\mathbf{q}} - \mu_{pair}), \quad (2)$$

where $b(x)$ is the usual Bose distribution function. The density of particles at radius r can be written as

$$n_{\sigma}(r) = \sum_{\mathbf{k}} [u_{\mathbf{k}}^2 f(E_{\mathbf{k}\sigma}) + v_{\mathbf{k}}^2 f(-E_{\mathbf{k}\bar{\sigma}})], \quad (3)$$

which depends on the coherence factors $u_{\mathbf{k}}^2$, $v_{\mathbf{k}}^2 = (1 \pm \xi_{\mathbf{k}}/E_{\mathbf{k}})/2$ with $\xi_{\mathbf{k}} = \epsilon_{\mathbf{k}} - \mu(r)$, $E_{\mathbf{k}\uparrow} = -h + E_{\mathbf{k}}$, and $E_{\mathbf{k}\downarrow} = h$

+ $E_{\mathbf{k}}$. The total number of particles and the polarization are, respectively, given by

$$N_{\sigma}(r) = \int d^3r n_{\sigma}(r), \quad N = N_{\uparrow} + N_{\downarrow}, \quad (4)$$

$$p = (N_{\uparrow} - N_{\downarrow})/N. \quad (5)$$

Our calculations proceed by numerically solving the self-consistent equations. Here we use N and p as input; these are the control parameters in experiment.

Figure 1 shows the behavior of the various gap parameters and the majority and minority spin components as a function of radius in the trap, for the case of a near-BEC system with $1/k_F a = 1.5$. The upper panels are for the normal phase and the lower panels are in the superfluid state. We present results for three different polarizations and focus first on the lower panels where there are two distinct components to the gap Δ_{sc} and Δ_{pg} . The two gap functions, Δ_{sc} and the total gap Δ , are plotted vs r along with the difference density for up and down spins, or alternatively, the polarization. We overlay these plots into order to show clearly what are the contributions to the polarization from the condensate (I), where $\Delta_{sc} \neq 0$, the correlated, but normal mixed region (II), where $\Delta_{sc} = 0$, but $\Delta \neq 0$, and noninteracting Fermi gas(s) regime (III), where $\Delta = 0$.

It can be seen that there is very little polarization present in the condensate (I) which appears below T_c , as has been inferred experimentally [1–3]. Rather, the bulk of the polarization is present in the correlated but normal region (II) in which there is a finite excitation gap Δ , but vanishing Δ_{sc} . In region III at even larger radii, Δ is essentially zero and region III is predominantly composed of the majority spin component. In this regime, one expects the cloud wing shape to be that of a noninteracting Fermi gas, and this provides the basis for a reasonable thermometry [3]. As T is lowered, the noncondensed pairs in region II will be converted into the condensate, thereby merging regions I and II.

Because we have not yet incorporated the $q_0 \neq 0$ correlations of the FFLLO state, in Figs. 1 and 2 the largest of three values of p used is associated with an instability at the very edge of the minority cloud. Nevertheless, since n_{\downarrow} essentially vanishes there, this is expected to have very little qualitative effect on our results.

The insets in the lower panel show the density profiles for the majority and minority component. Qualitatively similar to what has been observed experimentally [3], a small “kink” in the majority is present which we associate with the radius at which the condensate ends. The minority component contains a condensate central peak with a very long tail; this is then a thermally induced bimodal structure. The upper panel shows the behavior in the normal state, where the condensate $\Delta_{sc} = 0$. Nevertheless, it can be seen that an excitation gap Δ is present as long as $n_{\downarrow} \neq 0$. In this way the particle profiles do not correspond to those of a noninteracting gas, and the polarization is rather evenly distributed at all radii in the cloud. It may also be seen from these insets that as the system varies from above to below T_c , the profile of the minority component contracts into the center of the trap, as observed [3].

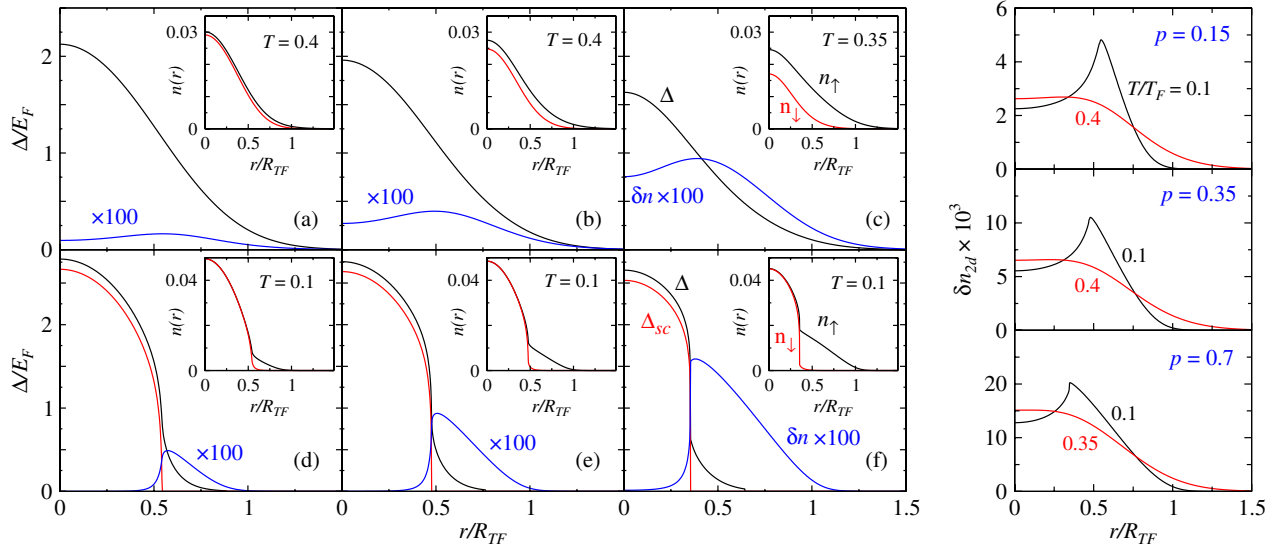


FIG. 1. (Color online) Spatial distribution of the excitation gap $\Delta(r)$ and order parameter $\Delta_{sc}(r)$ (main figures) and density $n_\sigma(r)$ (insets) at $1/k_F a = 1.5$ for the majority and minority fermions at different polarizations ($p=0.15, 0.35,$ and 0.7 from left to right) above (upper row) and below (lower row) T_c . Here $T_c/T_F \approx 0.36, 0.35,$ and $0.31,$ respectively. The density difference $\delta n(r)$ is shown in blue in the main figures, sharing the same vertical axis as $\Delta(r)$. The temperatures for the upper row are $T/T_F = 0.4, 0.4,$ and $0.35,$ respectively, and for the lower row $T/T_F = 0.1$. Shown on the far right is the difference in column density, $\delta n_{2d}(r)$, for the three polarizations above and below T_c . Here $E_F = \hbar^2 k_F^2 / 2m = k_B T_F$ is given by the Fermi energy for an unpolarized, noninteracting Fermi gas with the same total number N at $T=0$, and $R_{TF} = \sqrt{2E_F / m\omega^2}$ is the Thomas-Fermi radius. The units for n and δn_{2d} are k_F^3 and k_F^2 , respectively.

We present comparable figures for the unitary case in Fig. 2. Most of the observations made above for the near-BEC case apply at unitarity as well. Here, one can see from the insets, however, that the kink in the majority profile is less apparent. Finally, we turn to Fig. 3 where the counterpart plots are presented for the BEC regime with $1/k_F a = 3.0$. From the right column, it may be seen that polarization penetrates down to the trap center [20], when the overall polarization p is high. This is in agreement with the expectations from the homogeneous case [13].

It should be stressed that our calculations indicate that dramatic changes in the shape of the density profiles do not occur until T is substantially lower than T_c . This may explain why the experimentally observed T_c values are less [3] than those we compute. Also important is the fact that the mixed normal phase we find here (region II) is not related to that introduced at $T=0$ in other theoretical work [11,12], since we find very strong correlations between the different spin states. Moreover, the noncondensed pair contribution we consider has no counterpart at $T=0$. Indeed, there appears to

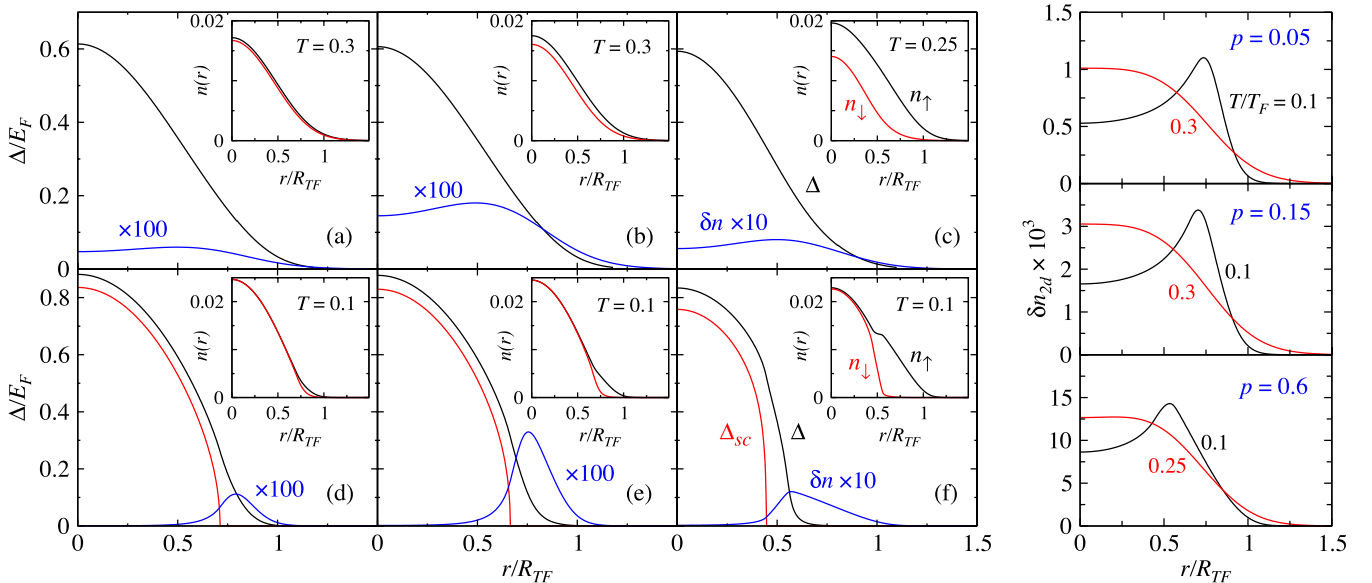


FIG. 2. (Color online) Same as Fig. 1, but at unitarity. From left to right, $p=0.05, 0.15,$ and $0.6,$ and $T_c/T_F \approx 0.27, 0.27,$ and $0.23,$ respectively. In upper row, $T/T_F = 0.3, 0.3,$ and $0.25;$ in lower row $T/T_F = 0.1$. On the far right is $\delta n_{2d}(r)$ above and below T_c .

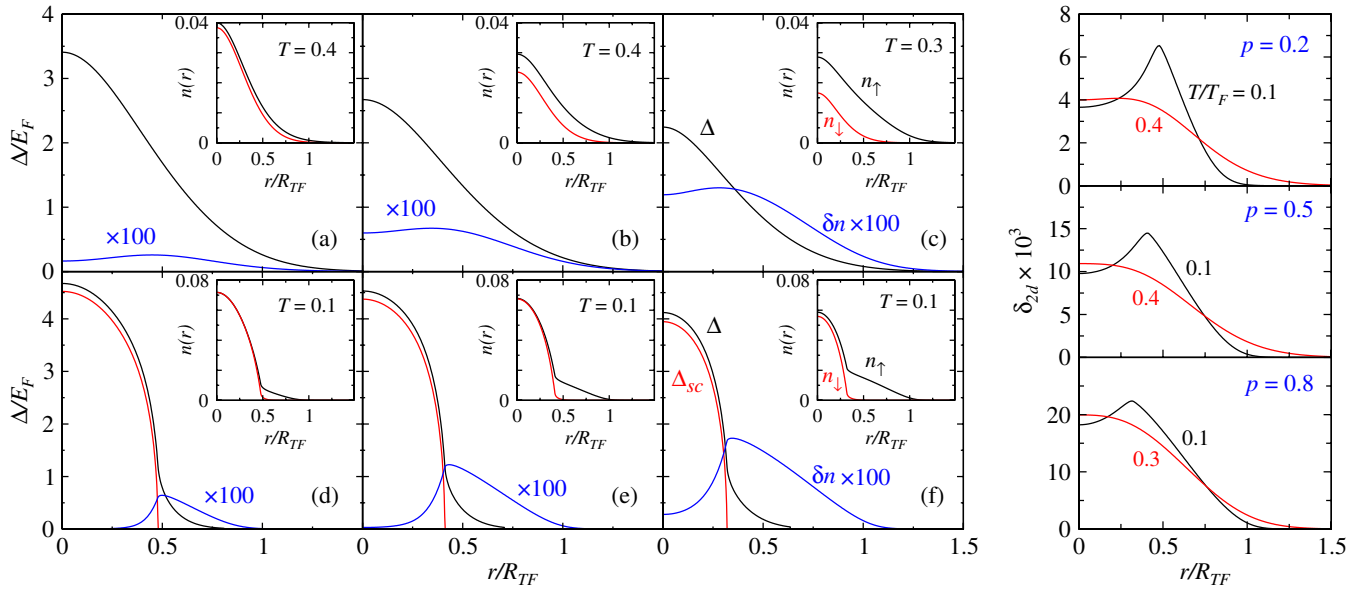


FIG. 3. (Color online) Same as Fig. 1, but for $1/k_F a = 3$. From left to right, $p = 0.2, 0.5$, and 0.8 , and $T_c/T_F \approx 0.39, 0.36$, and 0.28 , respectively. For the upper row, $T/T_F = 0.4, 0.4$, and 0.3 , respectively, and for the lower row $T/T_F = 0.1$. Shown on the far right is $\delta n_{2d}(r)$.

be no evidence from $T=0$ BdG investigations [15,16] for such a mixed normal phase.

Many of the qualitative observations reported in this paper correspond to their counterparts in Ref. [3]. One exception, however, is that in Ref. [3], it is noted that only regions I and III are present in the near-BEC regime, whereas we find for $T \neq 0$ all three regions appear, just as in the unitary case. Region II corresponds to the presence of noncondensed pairs, expected at finite T in the near-BEC regime. We find that after column integration of the density profile in Figs. 1–3, a double peaked structure emerges below T_c in the difference profile δn_{2d} , rather similar to that observed in ex-

periments [1,2]; this disappears above T_c . At a more quantitative level, our results at unitarity may change somewhat when we include FFLO condensate contributions and associated higher values of p . More importantly, as stressed in Ref. [3], our studies show that a significant fraction of the normal region in the trap contains strong interactions between the two spin states that we associate with the presence of noncondensed pairs and related [6] fermionic excitation (pseudogap).

This work was supported by NSF-MRSEC Grant No. DMR-0213745. We thank M.W. Zwierlein for useful communications.

- [1] M. W. Zwierlein, A. Schirotzek, C. H. Schunck, and W. Ketterle, *Science* **311**, 492 (2006).
- [2] G. B. Partridge, W. Li, R. I. Kamar, Y. A. Liao, and R. G. Hulet, *Science* **311**, 503 (2006).
- [3] M. W. Zwierlein, H. Schunck, A. Schirotzek, and W. Ketterle, *Nature (London)* **442**, 54 (2006).
- [4] A. J. Leggett, *Modern Trends in the Theory of Condensed Matter*, edited by A. Pekalski and J. Przystawa (Springer-Verlag, Berlin, 1980), pp. 13–27.
- [5] Q. J. Chen, I. Kosztin, B. Jankó, and K. Levin, *Phys. Rev. Lett.* **81**, 4708 (1998).
- [6] Q. J. Chen, J. Stajic, S. N. Tan, and K. Levin, *Phys. Rep.* **412**, 1 (2005).
- [7] D. E. Sheehy and L. Radzihovsky, *Phys. Rev. Lett.* **96**, 060401 (2006).
- [8] W. Yi and L. M. Duan, *Phys. Rev. A* **73**, 031604(R) (2006).
- [9] W. V. Liu and F. Wilczek, *Phys. Rev. Lett.* **90**, 047002 (2003).
- [10] M. M. Forbes, E. Gubankova, W. V. Liu, and F. Wilczek, *Phys. Rev. Lett.* **94**, 017001 (2005).
- [11] T. N. De Silva and E. J. Mueller, *Phys. Rev. A* **73**, 051602(R) (2006).
- [12] M. Haque and H. T. C. Stoof, e-print cond-mat/0601321.
- [13] C.-C. Chien, Q. J. Chen, Y. He, and K. Levin, *Phys. Rev. Lett.* **97**, 2006 (to be published).
- [14] J. Stajic, Q. J. Chen, and K. Levin, *Phys. Rev. Lett.* **94**, 060401 (2005).
- [15] J. Kinnunen, L. M. Jensen, and P. Torma, *Phys. Rev. Lett.* **96**, 110403 (2006).
- [16] K. Machida, T. Mizushima, and M. Ichioka, e-print cond-mat/0604339.
- [17] P. Fulde and R. A. Ferrell, *Phys. Rev.* **135**, A550 (1964); A. I. Larkin and Y. N. Ovchinnikov, *Zh. Eksp. Teor. Fiz.* **47**, 1136 (1964) *Sov. Phys. JETP* **20**, 762 (1965)].
- [18] L. Y. He, M. Jin, and P. F. Zhuang, e-print cond-mat/0606322.
- [19] C. H. Pao, S. T. Wu, and S. K. Yip, *Phys. Rev. B* **73**, 132506 (2006).
- [20] P. Pieri and G. C. Strinati, *Phys. Rev. Lett.* **96**, 150404 (2006).
- [21] I. Kosztin, Q. J. Chen, B. Jankó, and K. Levin, *Phys. Rev. B* **58**, R5936 (1998).
- [22] P. Pieri and G. C. Strinati, *Phys. Rev. Lett.* **91**, 030401 (2003).
- [23] J. Stajic, J. N. Milstein, Q. J. Chen, M. L. Chiofalo, M. J. Holland, and K. Levin, *Phys. Rev. A* **69**, 063610 (2004).
- [24] I. Kosztin, Q. J. Chen, Y.-J. Kao, and K. Levin, *Phys. Rev. B* **61**, 11662 (2000).